





## Article

# Melanin Pathway Determination in *Sclerotium cepivorum* Berk Using Spectrophotometric Assays, Inhibition Compound, and Protein Validation

Luis M. Salazar-García <sup>1</sup>, Rocío Ivette Ortega-Cuevas <sup>1</sup>, José A. Martínez-Álvarez <sup>1</sup>,  
Sandra E. González-Hernández <sup>1</sup>, Román Antonio Martínez-Álvarez <sup>1</sup>, Diana Mendoza-Olivares <sup>2</sup>,  
Miguel Ángel Vázquez <sup>2</sup>, Alberto Flores-Martínez <sup>1</sup> and Patricia Ponce-Noyola <sup>1,\*</sup>

<sup>1</sup> Departamento de Biología, División de Ciencias Naturales y Exactas, Campus Guanajuato, Universidad de Guanajuato, Guanajuato 36050, Mexico; lm.salazar@ugto.mx (L.M.S.-G.); ri.ortegacuevas@ugto.mx (R.I.O.-C.); martinezjose@ugto.mx (J.A.M.-Á.); se.gonzalez@ugto.mx (S.E.G.-H.); romanmartinez0510@gmail.com (R.A.M.-Á.); floralb@ugto.mx (A.F.-M.)

<sup>2</sup> Departamento de Química, División de Ciencias Naturales y Exactas, Campus Guanajuato, Universidad de Guanajuato, Guanajuato 36050, Mexico; dianam@ugto.mx (D.M.-O.); mvazquez@ugto.mx (M.Á.V.)

\* Correspondence: poncep@ugto.mx



**Citation:** Salazar-García, L.M.; Ortega-Cuevas, R.I.; Martínez-Álvarez, J.A.; González-Hernández, S.E.; Martínez-Álvarez, R.A.; Mendoza-Olivares, D.; Vázquez, M.Á.; Flores-Martínez, A.; Ponce-Noyola, P. Melanin Pathway Determination in *Sclerotium cepivorum* Berk Using Spectrophotometric Assays, Inhibition Compound, and Protein Validation. *Microbiol. Res.* **2022**, *13*, 152–166. <https://doi.org/10.3390/microbiolres13020013>

Academic Editor: Elisa Bona

Received: 22 February 2022

Accepted: 26 March 2022

Published: 29 March 2022

**Publisher's Note:** MDPI stays neutral with regard to jurisdictional claims in published maps and institutional affiliations.



**Copyright:** © 2022 by the authors. Licensee MDPI, Basel, Switzerland. This article is an open access article distributed under the terms and conditions of the Creative Commons Attribution (CC BY) license (<https://creativecommons.org/licenses/by/4.0/>).

**Abstract:** *Sclerotium cepivorum* Berk is the etiological agent of white rot disease that affects plants of the genus *Allium*. This fungus produces resistance structures called sclerotia that are formed by a rolled mycelium with a thick layer of melanin and it can remain dormant for many years in the soil. Current interest in *S. cepivorum* has arisen from economic losses in *Allium* crops in the agricultural sector. Melanin is a component that protects the sclerotia from adverse environmental conditions. In many organisms, it plays an important role in the infectious process; in *S. cepivorum*, the pathway by which this component is synthesized is not fully described. By using infrared spectrophotometric assays applied direct to the sclerotia and a melanin extract followed by an NMR analysis and a tricyclazole melanin inhibition experiment, it allowed us to determine the dihydroxynaphthalene (DHN)-melanin pathway by which *S. cepivorum* performs its melanin synthesis. Moreover, we focused on studying scytalone dehydratase (SDH) as a key enzyme of the DHN-melanin synthesis. We obtained the recombinant SDH enzyme and tested its activity by a zymogram assay. Thereby, the *S. cepivorum* melanogenic route was established as a DHN pathway.

**Keywords:** melanin; DHN; FTIR; NMR; sclerotia; scytalone dehydratase; white rot; *Sclerotium cepivorum* Berk

## 1. Introduction

*Sclerotium cepivorum* is a pathogenic fungus of plants from the *Allium* genus such as garlic and onion that causes the disease known as white rot [1]. *S. cepivorum* usually grows on moldy soils generating hyphae and sclerotia [2]. Despite the relevance of *Allium* cultures and their losses because of white rot, advances in the biological knowledge of *S. cepivorum* are limited, especially those directed toward the study of sclerotia.

Sclerotia are nutrient-rich structures produced by many fungi that allow them to remain dormant or quiescent during unfavorable conditions. When conditions improve, the sclerotia germinate in order to propagate the pathogenic fungus [3]. Sclerotia structures comprise a rolled mycelium covered by an outer layer of melanin, forming a ring over the hyphae tissue [4]; this helps the sclerotia to survive on the soil for several years [2]. *S. cepivorum* produces sclerotia as a resistance form and for that reason, controlling white rot disease has been difficult. Physical, chemical, and biological methods have not been completely effective in reducing attacks of *S. cepivorum* on *Allium* crops [5].

*S. cepivorum* sclerotia are the initial source of the infective inoculum and can remain viable for up to 20 years in the soil; this resistance is attributed to the blackish layer of melanin that covers it [6]. Melanin in fungi protects against physical and chemical environmental factors such as oxidative stress, UV radiation, desiccation, cold, high humidity, heat, and antagonistic micro-organisms [7,8]. In a related organism, *Magnaporthe oryzae* (*Pyricularia oryzae*), a mutant lacking a melanin expression was reported to be more sensitive to stress factors [9]. In *Sclerotinia sclerotiorum*, a fungus with a high evolutionary similarity to *S. cepivorum* [10,11] and notable for its wide host range and environmental persistence, a melanin deficiency affected the sclerotium development but not its pathogenicity [7,12].

Melanin in fungi has been divided into three different categories: dihydroxyphenylalanine, also called DOPA-melanin, eumelanin, or the tyrosine route [13,14]; a variant named pyromelanin produced from the precursor glutaminyloxybenzene (GBH-melanin) [14]; and dihydroxynaphthalene-melanin, also known as DHN-melanin, allomelanin, the DHN pathway, or the polyketide pathway [13,15]. Although a feasible strategy for combating white rot disease is to inhibit *S. cepivorum* melanization, this pathway is not well-established and alternatives for its control are still limited [4,16]. The study of the basic biology of *S. cepivorum* and several biological processes such as the development of the sclerotia and the melanization pathway will help to understand the mechanisms responsible for white rot disease and thus lay the foundations for the development of strategies that allow the control of the infection [2].

Here, we present chemical and molecular evidence that allow us to suggest that the melanin synthesis in *S. cepivorum* is by the DHN pathway. We used infrared spectrophotometric assays and nuclear magnetic resonance (NMR) to produce an initial proposal of the produced melanin. These studies were supported by the use of tricyclazole, which specifically interferes with DHN melanization [17]; the treated strains showed a delayed melanin formation. In the annotation of the *S. cepivorum* genome, we identified several genes that take part in the DHN-melanin synthesis pathway, of which scytalone dehydratase (SDH) is a key enzyme. To complete this study, the identification of the open reading frame (ORF) of the gene encoding of the SDH protein was carried out, expressed in a yeast system, and the activity of the recombinant protein was measured. This protein has important roles in the development and morphology of fungi related to *S. cepivorum* [12,18] and in this research we demonstrate the importance it plays in the synthesis of melanin. In addition, the SDH protein could be considered a potential target for the control of white rot disease in plants of the *Allium* genus.

## 2. Materials and Methods

### 2.1. Micro-Organisms and Culture Media

*S. cepivorum* SC strain (isolated by Dr. D. Guzmán-de-Peña, CINVESTAV-Irapuato, Guanajuato, Mexico) was used in this research. The strain was grown on potato dextrose agar (PDA) plates at 18 °C; for the sclerotia recovery, the time of incubation was 13–17 days. The sclerotia were harvested by mechanical means and kept at room temperature until used. The mycelium was obtained by incubating the sclerotia on PDA plates with a cellophane membrane for 3–7 days at 18 °C. It was then harvested by mechanical means and used immediately or kept at –20 °C until used. *Pichia pastoris* X-33 strain cells were grown in a yeast extract peptone dextrose (YPD) medium (1% w/v yeast extract, 2% w/v gelatin peptone, and 3% w/v dextrose) or YPDS (YPD plus 1 M Sorbitol); for the *Magnaporthe grisea* 70-15 strain (Orbach M., University of Arizona), the strain cells were propagated in a potato dextrose broth medium (PDB) for 5 days at 120 rpm in an orbital incubator at 28 °C. An *Escherichia coli* DH5 $\alpha$  strain for cloning was grown on a Luria Bertani (LB) medium with appropriate antibiotics [19].

### 2.2. Sclerotia Melanin Extraction

*S. cepivorum* was grown for 13–17 days on PDA plates to promote the sclerotia development. The sclerotia were harvested by mechanical means and collected in a sterile

container. Two equivalent volumes of distilled water were then added and strongly shaken in a vortex for 10 min to remove any mycelium residue from the surface of the sclerotia. The suspension was left to stand until the sedimentation of the sclerotia and the supernatant was removed. The sclerotia were washed twice in the same way and dried for 48 h at 40 °C. The recovered sclerotia were mixed with an equivalent volume of chloroform and strongly shaken in a vortex for 10 min. The sedimented sclerotia were recovered and solvent evaporation was promoted by a laminar flow. The dry sclerotia were directly used (direct sample) for the melanin extraction or kept at room temperature until use. The melanin extraction was performed as described by Gadd [20] but with slight modifications. The sclerotia obtained from the direct sample were ground in a mortar, resuspended in three equivalent volumes of 3 M NaOH, mixed thoroughly in a vortex for 10 min and incubated for 48 h at 60 °C. The homogenate was centrifuged at room temperature for 10 min at  $12,000 \times g$  and the supernatant containing the melanin was recovered. The melanin was precipitated by adding 1 M HCl until a pH of 2.0 was obtained; this was then centrifuged for 20 min at  $15,000 \times g$ . The supernatant was removed, and the precipitate was washed 4 times with distilled water and centrifuged for 10 min at  $12,000 \times g$ . The melanin pellet was washed with chloroform, stirred slightly, and placed in a laminar flow until solvent evaporation; once dried, the purified preparation was kept at room temperature.

### 2.3. Analysis of the Melanin Composition

Direct samples of the sclerotia and the purified extracted melanin were analyzed by a Fourier transform infrared spectrophotometer (FTIR) in a Perkin Elmer SPECTRUM 100 infrared spectrophotometer by using a diamond attenuated total reflectance (ATR) device at a resolution of  $4 \text{ cm}^{-1}$  in the wavenumber region of  $4000\text{--}650 \text{ cm}^{-1}$ . The purified melanin was analyzed by  $^{13}\text{C}$  NMR in a solid state by using a Bruker Avance III HD 400 MHz instrument operating at a frequency of 100.613 MHz employing  $\text{ZrO}_2$  rotors of 4 mm OD and 50  $\mu\text{L}$ . The cross-polarization (CP) technique was applied during the magic-angle spinning (MAS) of the rotor at 10 kHz; 60,000 scans were accumulated (26 h) and the data were processed in MestreNova software version 6.

### 2.4. Susceptibility of *S. cepivorum* to Tricyclazole

The *S. cepivorum* susceptibility test was developed as previously described by Froyd et al. but with slight modifications [21]. Briefly, PDA discs (6 mm) containing the *S. cepivorum* mycelium were inoculated on PDA plates with two doses of tricyclazole (SIGMA-ALDRICH™, CAS number 41814-78-2, Burlington, MA, USA), one high (400  $\mu\text{g}/\text{mL}$ ) and one low (100  $\mu\text{g}/\text{mL}$ ) using a concentrated tricyclazole solution (10 mg/mL in absolute ethanol). Two control samples were used; the first contained absolute ethanol and the other contained neither alcohol nor tricyclazole. The number of sclerotia produced was counted at day 13 post-inoculation by using a Stratagene Eagle Eye II Imaging System™. Three independent experiments with duplicates were performed and an ANOVA statistical analysis was used to describe the data.

### 2.5. Isolation of *S. cepivorum* DNA, RNA, and cDNA

DNA was isolated as reported by Raeder and Broda [22], using the mycelium grown on PDA plates for four days. The DNA obtained was washed with 70% (*v/v*) ethanol and kept at  $-70 \text{ }^\circ\text{C}$  until used. The total RNA was isolated with TriZol™ and the cDNA was synthesized following a protocol previously standardized in a laboratory [23].

### 2.6. Expression of *S. cepivorum* SDH Protein in *P. pastoris* (X-33) Cells

SDH cDNA was amplified by using the D4 forward primer 5' CTGCAGCATCCACTATGGCTCAAGACAGAATTTCTTTTG-3 and the R6 reverse primer 5'-GCGGCCGCGTACTGCTTAAACCCCCCTTAAAAACC-3' (underlined bases indicate *Pst*I and *Not*I sites, respectively; see extended data in Supplementary Table S1) to yield a 522 bp amplicon. The amplicon was cloned into pCR2.1-TOPO (Invitrogen™), Waltham, MA, USA) and then

subcloned into the *Pst*I and *Not*I sites of pPICZ $\alpha$ B (Invitrogen<sup>TM</sup>), generating pPICZ $\alpha$ B/*sdh*. As the vector conferred a resistance to Zeocin<sup>TM</sup>, *P. pastoris* transformant cells were selected in a YPD medium supplemented with 100  $\mu$ g/mL of Zeocin<sup>TM</sup>. The production of the recombinant protein was achieved by growing the methylotrophic yeast cells in a buffered methanol-complex medium (BMMY) (1% yeast extract, 2% casein peptone, 100 mM potassium phosphate, pH 6.0, 1.34% bacto-yeast nitrogen base (YNB) *w/v*,  $4 \times 10^{-5}$ % biotin *w/v*, 1% glycerol *v/v*,  $4 \times 10^{-3}$ % histidine *w/v*) and the expression was induced with methanol to a final concentration of 1% following Pichia Expression Kit (ThermoFisher EasySelect<sup>TM</sup>, Waltham, MA, USA). The purification of the SDH recombinant was performed by using Ni-NTA Sepharose (1 mL column, eluted by gravity) for the purification of the poly histidine-containing recombinant proteins (Life Technologies<sup>TM</sup>, Grand Island, NY, USA) following the instructions provided by the manufacturer. The protein was analyzed by 12% SDS-PAGE stained with Coomassie brilliant blue as reported by Laemmli [24].

### 2.7. Zymogram Assay for Recombinant SDH Activity

Native polyacrylamide gel electrophoresis was performed by using 10% acrylamide gel in a Tris–boric–EDTA (8.9 mM Tris base, 8.9 mM boric acid, 0.2 mM EDTA) buffer with a pH of 8.0 as reported by Laemmli [24]. Once the electrophoresis finished, the gel was incubated for 30 min with 25  $\mu$ M fluorinated coumarin, an SDH substrate (Ethyl-2-hydroxy-2-(trifluoromethyl)-2H-chromene-3-carboxylate; see Supplementary Material File S1 and Supplementary Figures S1–S3). The SDH activity was registered by using Chemi Doc (BIORAD<sup>TM</sup>) equipment with a fluorescence filter for SyBr Green<sup>TM</sup> with 2 s of exposure. The cell extracts of *M. grisea* 70-15 were used as a positive control for the enzyme activity.

### 2.8. Cell extract Obtention from *Magnaporthe grisea*

The protocol was based on Wheeler [25] with slight modifications. *M. grisea* mycelium growth of 7 days in PDA was collected, transferred to 100 mL of PDB, and incubated for 72 h at 28 °C with stirring at 180 rpm. The mycelium was harvested by filtration, washed with Na<sub>3</sub>PO<sub>4</sub> 0.1 N, pH 7, mixed with glass beads and placed in an MSK Braun homogenizer. The bottle was filled to one third of the volume with glass beads, a second third with the mycelium in a 0.1 N Na<sub>3</sub>PO<sub>4</sub> buffer, pH 7, and subjected to disruption under the following conditions: 5 s with CO<sub>2</sub> and 15 s without CO<sub>2</sub>. This was repeated 6 times. The sample was centrifuged at 3000  $\times$  g for 5 min to recover the cell-free extract (supernatant).

### 2.9. Microscopy Images

The fungal cells and sclerotia were examined by microscopy using a Zeiss<sup>TM</sup> microscope and an Axiocam MRc camera. All images were captured by using the same exposure settings (white light).

## 3. Results

### 3.1. Spectroscopy-Based Analysis of Pigment Extracted from *S. cepivorum*

An FTIR was used to analyze the *S. cepivorum* melanin and to provide an initial insight into its pathway. The IR analysis by diamond ATR was used to facilitate the handling of these solid compounds and we obtained the sclerotia- and melanin-extracted spectra; both were compared by overlapping, obtaining similar spectra where the most important signals were present in both samples (Figure 1).

The spectra were analyzed, and their peaks were described to characterize the specified bonds and chemical groups (Table 1). The different products generated during the melanin synthesis made it possible to realize an initial suggestion to differentiate between the melanogenic pathways involved [26] among the signals; those located at 3300 cm<sup>-1</sup>–3000 cm<sup>-1</sup> could help to make a proposal because in the DOPA-melanin route, a sharp peak of medium intensity is characteristic of nitrogen functional groups [27] and this did not appear and the wide and high-intensity peak could be associated with the hydroxyl group in the DHN pathway (Table 1) [26,28,29].

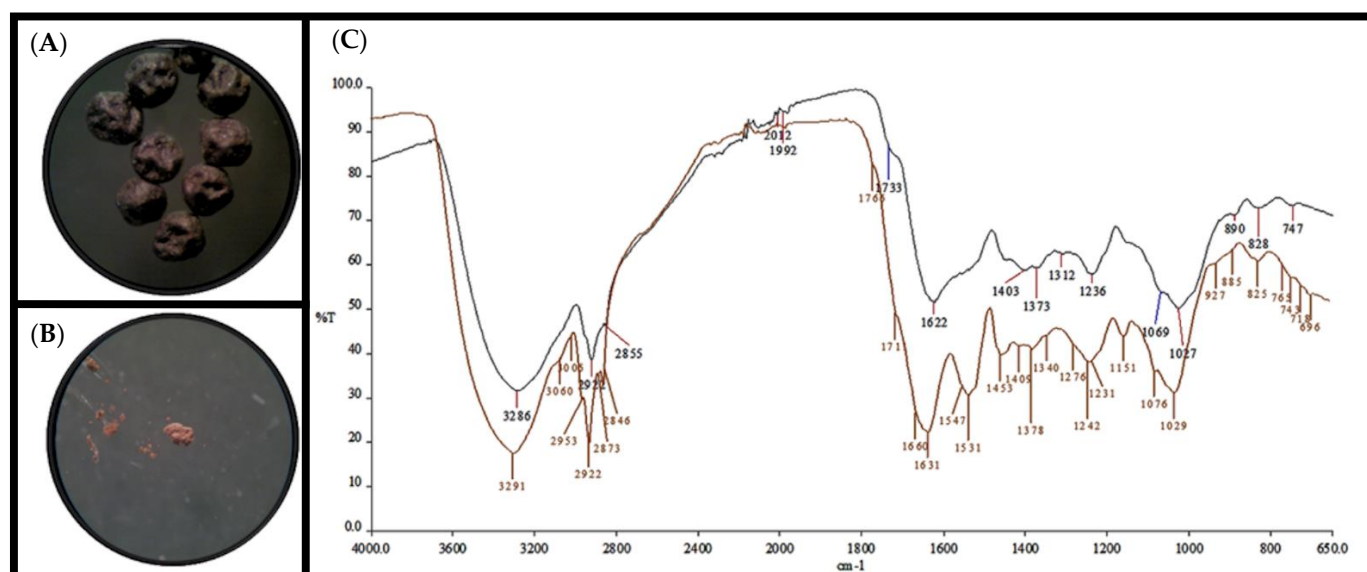


**Figure 1.** Overlapping FTIR spectra. (A) Direct sample and (B) purified melanin compound obtained from *S. cepivorum* sclerotia. The images were obtained by using a stereoscope. (C) Spectra obtained by FTIR in diamond ATR of the direct sample (black) and of the purified melanin compound (brown); the principal signals are annotated. Spectra were performed with a diamond ATR attachment Perkin Elmer SPECTRUM 100 infrared spectrophotometer (resolution of 4 cm<sup>-1</sup> in the number region of 650 cm<sup>-1</sup> to 4000 cm<sup>-1</sup>).

**Table 1.** Melanin *S. cepivorum* IR signals. Spectra signals of the purified compound and the direct preparation, both from *S. cepivorum* sclerotia. Identification based on Pretsch tables of spectral data for structure determination of organic compounds [28].

Purified Compound		Direct Sample	
Frequency (cm <sup>-1</sup> )	Signal Generating Group	Frequency (cm <sup>-1</sup> )	Signal Generating Group
3291	-O-H Elongation vibration. Polymeric association.	3286	-O-H Elongation vibration. Polymeric association.
3060 3005 2953	=C-H Elongation vibration. Aromatic compound.	2922	=C-H Elongation vibration. Aromatic compound.
1631 1547 1531 1453	-C=C- Deformation (in plane) aromatic compound.	1622	-C=C- Deformation (in plane) aromatic compound.
1409 1378	-C-O Elongation vibration. Characteristic of phenol and derivatives.	1403 1373	-C-O Elongation vibration. Characteristic of phenol and derivatives.
1242	-O-H Deformation (in plane). Characteristic of phenol and derivatives.	1236	-O-H Deformation (in plane). Characteristic of phenol and derivatives.
1151 1076 1029	-C-H Deformation (in plane) and aromatic ring substitution 1:2:3.	1069 1027	-C-H Deformation (in plane) and aromatic ring substitution 1:2:3.
885 765 718	-C-H Deformation (out plane) and aromatic ring substitution 1:2:3.	890 828 747	-C-H Deformation (out plane) and aromatic ring substitution 1:2:3.

A <sup>13</sup>C RMN technique was used to complement our FTIR results and support the initial proposal about the DHN-melanin pathway. The purified melanin was ground again, and 75 mg was placed and compacted in a rotor (ZrO<sub>2</sub>, 4 mm OD); the spectrum is depicted

in Figure 2. The  $^{13}\text{C}$  spectrum data are described in Table 2 and the prediction of the chemical shifts of the carbons presented in the dimers of 1,8 dihydroxynaphthalene was made according to Manini and collaborators [30] by using MestreNova software version 6. The prediction was made because the literature did not report a  $^{13}\text{C}$  NMR spectrum in the solid state of melanin produced by a fungus through the 1,8 DHN source that was free of other components of the cell wall such as the residues of proteins, chitin, polysaccharides, or lipids.

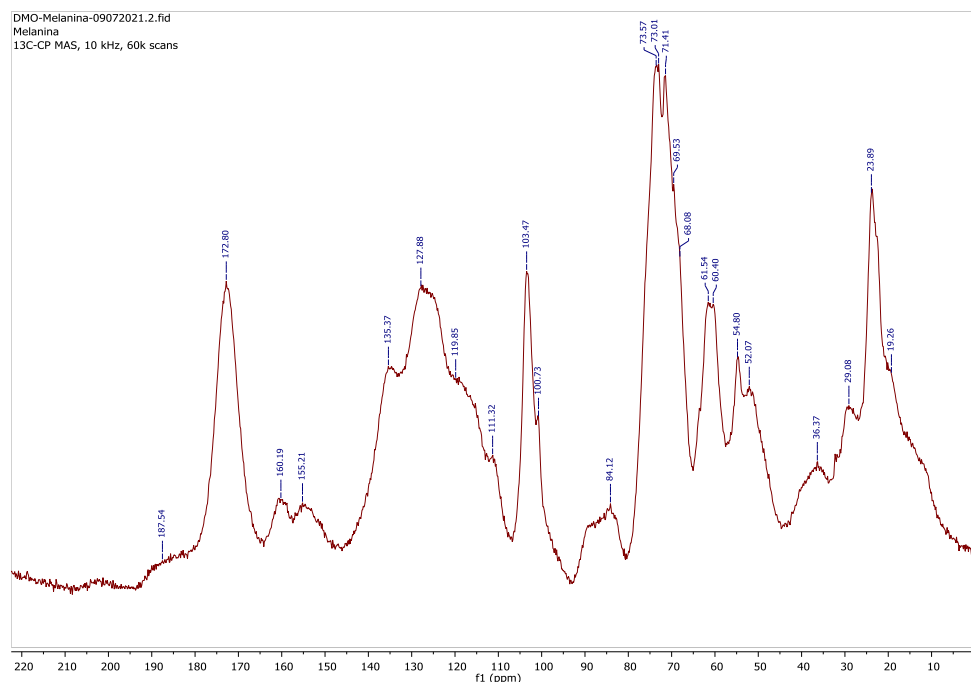


**Figure 2.** Purified melanin  $^{13}\text{C}$  NMR spectrum of *S. cepivorum* Berk (400 MHz).

**Table 2.**  $^{13}\text{C}$  NMR resonance assignments for *S. cepivorum*-extracted melanin.

Chemical Shift, ppm	Chemical Grouping	Reference Materials	Literature Refs.
172.80	-CONH	Chitin	[31,32]
160.19	Aromatic -C-, O-naphthyl	Poly 1,8 DHN	[31]
135.77–111.32	Aromatic -C-, -C=C-	Poly 1,8 DHN, likely oleoyl	[31,33]
103.47, 100.73	Aromatic -C-, -O-CH-O-	Chitin, glucan	[32]
84.12	-CHOH	$\alpha$ -1.3 glucan	[32]
73.57–71.41	-CHOH, -CHO-	Chitin, $\alpha$ -1.3 glucan	[32]
61.54	-CH <sub>2</sub> OH	Chitin	[32]
60.40	-CH <sub>2</sub> OH	$\alpha$ -1.3 glucan	[32]
54.80	-CH-NH-	Chitin	[32]
29.08	-(CH <sub>2</sub> )- (C4–C7, C2–C16)	Likely oleoyl	[33]
23.89	-C(=O)-CH <sub>3</sub> , -(CH <sub>2</sub> )- (C3)	Chitin, likely oleoyl	[32,33]

### 3.2. *S. cepivorum* Melanization Is Affected by Treatment with Tricyclazole

Tricyclazole has been used against rice blast caused by *M. grisea* [34]; this compound acts as a competitive inhibitor of the reduction complex formed between the 3-hydroxynaphthalene reductase, a specific enzyme in the DHN pathway, with nicotinamide adenine dinucleotide phosphate (NADPH) in the melanin synthesis [17,25].

In laboratory conditions, the sclerotia development started at 9 days on a PDA plate at 18 °C. The effect of tricyclazole on the *S. cepivorum* growth showed atypical sclerotia development, unlike that observed in the controls (Figure 3A). When 100  $\mu\text{g}/\text{mL}$  of tricyclazole was used, the sclerotia presented an uncommon coloration and when a concentration of 400  $\mu\text{g}/\text{mL}$  of the tricyclazole was used, the sclerotia did not melanize. On day 13,

the sclerotia pigmentation was not completely present in the assays with 100 µg/mL and 400 µg/mL of tricyclazole (Figure 3B).

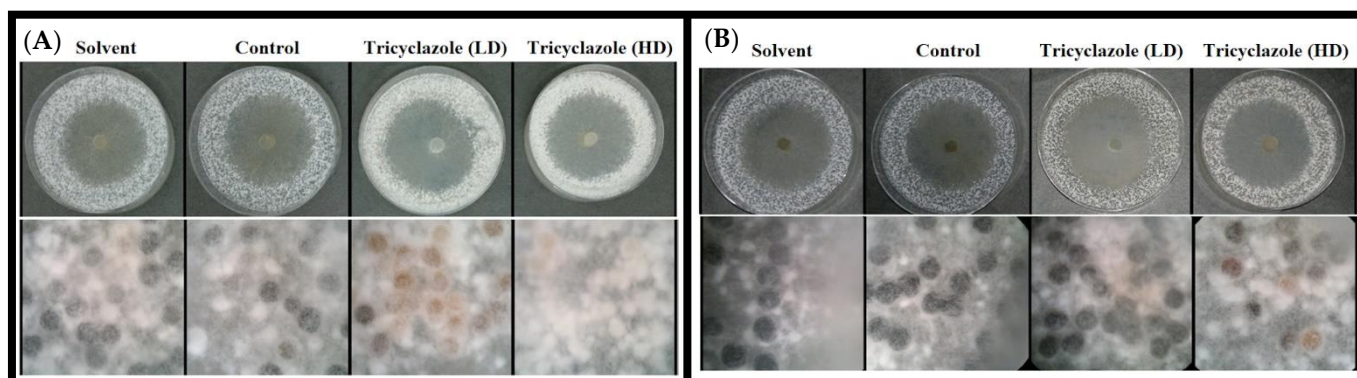


**Figure 3.** Melanization delay by tricyclazole in *S. cepivorum*. (A) Sclerotia at day 9 of growth and (B) sclerotia at day 13 of growth; top panels represent the Petri dishes, and the bottom panels represent the stereoscopic photographs of sclerotia. LD = 100 µg/mL tricyclazole; HD = 400 µg/mL tricyclazole.

The quantification of the sclerotia number was performed on day 13 by using a Stratagene Eagle Eye II Imaging System <sup>TM</sup> based on the opacity and spherical shape of the samples; therefore, we associated the inhibition caused by tricyclazole when the sclerotia showed an effect in the melanization, delayed pigmentation time, and reduced number of pigmented sclerotia formations compared with the controls (Figure 4). In this way, the effect of tricyclazole on the melanization of the sclerotia from *S. cepivorum* was evaluated. The results showed that tricyclazole delayed the melanization of the sclerotia, suggesting—together with the FTIR and NMR data—that the melanization of the *S. cepivorum* sclerotia was through the DHN-melanin pathway as well as *S. sclerotiorum* [7].

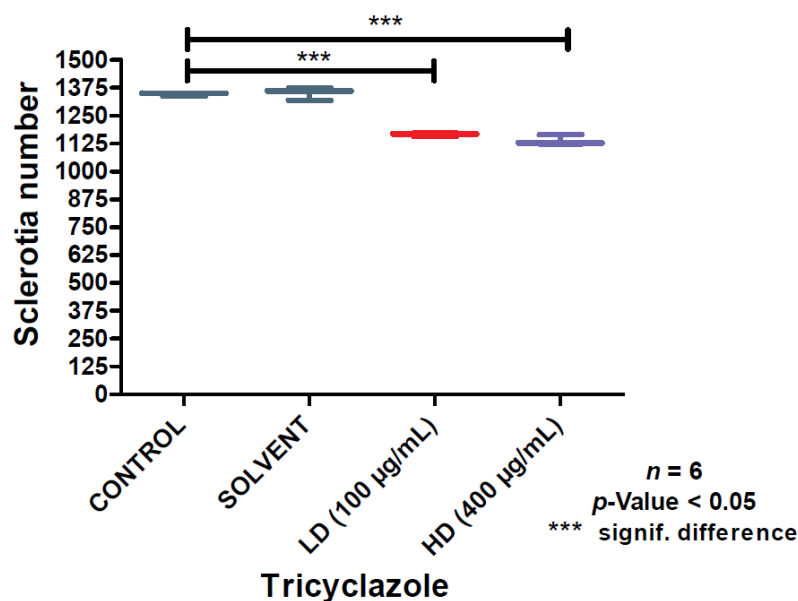


**Figure 4.** Effect of tricyclazole on *S. cepivorum* sclerotia melanization. Box and whiskers graph; the sclerotia were analyzed by using a Stratagene Eagle Eye II Imaging System <sup>TM</sup> on day 13 post-inoculation. ANOVA statistical analyses from 3 independent experiments were performed in duplicate. \*\*\*  $p < 0.05$ .

### 3.3. Identification and Obtainment of a *S. cepivorum* Scytalone Dehydratase Gene

Once the possible DHN melanization pathway in *Sclerotium cepivorum* was established, we focused on the enzymatic pathway reported for this molecule [35]. We were interested

in the scytalone dehydratase protein (SDH) because of its two-step participation in the melanization pathway [35]. We obtained the open reading frame (ORF) of the protein by sequencing the strain genome (*S. cepivorum* UGTO-Sc1) and comparing this with the reported genome (*S. cepivorum* GCA\_014898415 and GCA\_002162485); SDH ORF was deposited (GenBank: MK965546.1).

We compared the reported sequences of SDH and found high conserved regions in 5' but a variable length in the 3' regions even for other SDHs of *Sclerotinia sclerotiorum* strains (Supplementary Figure S4), indicating variations in this protein among the same species. We also compared our SDH sequence with several other SDHs reported in *S. cepivorum* strains and obtained a high alignment score in the nucleotide sequences (Supplementary Figure S5). A distance tree using the aa sequence indicated a relationship with *Sclerotinia sclerotiorum*, with an SDH of 167 amino acids (GenBank: APA08377.1) and a relationship with the SDH of the *Botrytis* species (Supplementary Figure S6). Furthermore, a phylogenetic tree based on our SDH aa sequence (GenBank: QJQ72301.1) compared with the reported sequences was constructed, revealing the relation with other fungi SDHs (Supplementary Figure S7).

A bioinformatics analysis specifically indicated a cluster of genes involved in the melanin synthesis such as the SDH, 1,3,8-naftalen thiol reductase, transcription factor Cys6, a transcription factor with C6 finger domains, and an alpha-beta hydrolase, which were also reported in *Alternaria alternata*, *Botrytis cinerea*, and *S. sclerotiorum* [36]. We cloned the cDNA of the *sdh* gene into the pPICZ $\alpha$ B vector to generate the construct pPICZ $\alpha$ B/*sdh*. The transformed *P. pastoris* X-33 cells were analyzed to verify the correct integration of the construct pPICZ $\alpha$ B/*sdh* into the yeast genome by using different pairs of primers (Supplementary Table S1). A 1115 bp amplicon (AOX-F and AOX-R primers were used) confirmed the complete integration of the construct in the yeast genome. The *sdh* amplicon of 522 pb was verified with D4 and R6 primers (Supplementary Figure S8).

Finally, to ensure the protein expression and to corroborate that the cDNA of *sdh* was in phase, the amplicon obtained with the AOX primers was sequenced, validating the correct insertion of the *sdh* cDNA. Once the positive clone was selected, the expression of the SDH was performed (Figure 5). We annotated the SDH protein in the GenBank database (accession number MK965546.1).

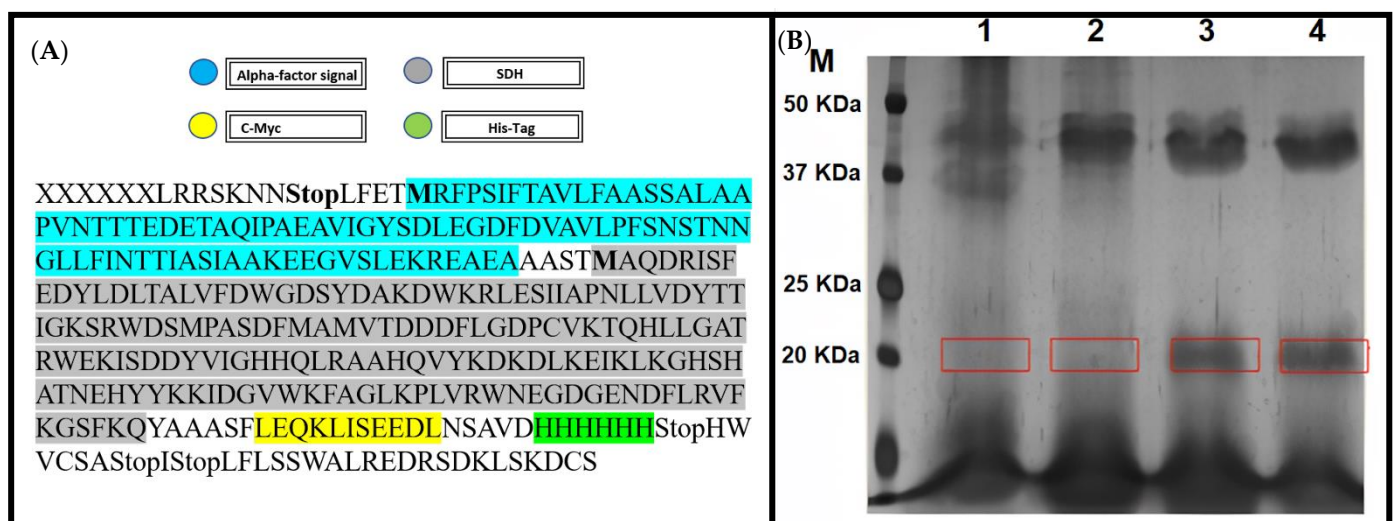


**Figure 5.** SDH *S. cepivorum* expression. (A) Scytalone dehydratase ORF, a protein with 167 amino acids and a tail of six histidines and C-Myc = cutting site. (B) SDH expression 1: *P. pastoris* wt; 2: *P. pastoris* with empty vector; 3 and 4: *P. pastoris* with SDH gene vector. SDH = 22.61 kDa (SDS-PAGE 12%, Coomassie staining).



### 3.4. *S. cepivorum* Scytalone Dehydratase Recombinant Activity

The SDH has a key role in melanin synthesis because it catalyzes two steps in the DHN-melanin pathway [37,38]. We induced the SDH heterologous expression in *P. pastoris* [39]. The recombinant SDH protein was analyzed by electrophoretic mobility under native conditions and its activity was revealed by using a fluorinated coumarin (Supplementary Material File S1). A zymogram assay (Figure 6) showed the activity of the recombinant SDH. *M. grisea* SDH was used as a positive control for the enzymatic activity [37,40].

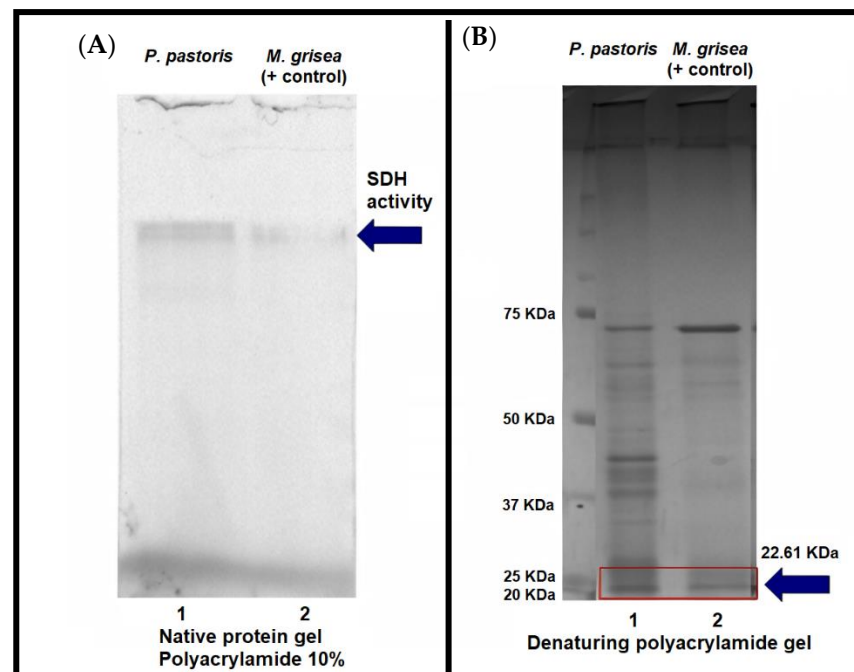


**Figure 6.** Scytalone dehydratase activity. Zymogram and SDS-PAGE of the recombinant scytalone dehydratase expressed in *P. pastoris*. (A) Zymogram, line 1: crude culture supernatant from *P. pastoris* transformed with pPICZ $\alpha$ B/*sdh*; line 2: positive activity control, *M. grisea* protein extracts, SDH detected activity is indicated. (B) SDS-PAGE: Proteins recovered from zymogram analysis; line 1, recombinant SDH protein (22.61 kDa); line 2, positive control from *M. grisea*.

## 4. Discussion

Melanin is an important compound in fungi protection against several factors such as UV radiation and dehydration as well as chemical and mechanical stressors [10,41]. It also protects against lytic enzymes produced by soil microbes [42] and it can be a determinant of virulence [43]. As aforementioned, melanin is a critical compound for fungi cells; for instance, its presence is necessary to develop appressorium in *M. grisea* [43] and for lifespan in *S. sclerotiorum* [7,12]. It has been inferred that *Sclerotium cepivorum* could have the same melanin synthesis route as *S. sclerotiorum* because of its evolutionary closeness [17]. Nevertheless, the lifecycle of *S. sclerotiorum* and its plant pathogenesis is different from the life cycle and plant pathogenesis of *S. cepivorum*. Melanin deficiency affects sclerotium development but not its pathogenicity [7,12]. However, for *S. cepivorum*, a deficiency in melanin production will affect the maturation of the sclerotia, impacting on its ability to resist changes in the environment and remain viable in the soil for long periods [44]. *S. cepivorum* is an exclusive pathogen of plant of the genus *Allium* (such as garlic, onion, scallion, shallot, leek, and chives) because of the germination signals that the sclerotia detect from plant-secreted sulfur compounds [1], hence the importance of knowing the melanin biosynthesis pathway in *S. cepivorum* as a possible control mechanism for white rot disease in *Allium* plants.

SDH is a key enzyme in melanin biosynthesis by the DHN pathway and SDH has been studied in different fungi such as *M. grisea* [43], *Bipolaris oryzae* [45], and *S. sclerotiorum* [7,12]. There are no specific reports of SDH in *S. cepivorum*, a fungus that belongs to the sclerotinacea family. There is a study by Wheeler [25] where the effect of tricyclazole on the melanin synthesis of mycelium homogenates of *S. cepivorum* was determined; a strong in vitro inhibition of 1,3,6,8-THN to scytalone was obtained and an accumulation of other melanin intermediates (using 159  $\mu\text{M}$  of tricyclazole) established that the dehydration reaction of scytalone and vermelone was not affected by tricyclazole. Melanin synthesis inhibition in *Monilia fructicola* causes the sclerotia, mycelia, and spores to be less environmentally persistent [46]. In *M. grisea*, the presence of inhibitors of the DHN pathway such as tricyclazole could not penetrate the host [47] and it also lost its pathogenicity and its virulence decreased [43]. Given the importance of melanin and the poorly studied melanin synthesis pathway in *S. cepivorum*, we were interested to know the route to improve the knowledge of this phytopathogenic fungus. IR spectroscopy was used to identify the functional groups of compounds and we used this to obtain initial insights to enable us to discriminate between the two melanins. The DOPA-melanin pathway is more common in *Basidiomycetes* whereas *Ascomycetes* use the DHN-melanin pathway and the final compounds have differential signal groups [48]. We used an FTIR to analyze the sclerotia pigment, taking advantage of the properties of melanin such as being soluble in alkali solutions, insoluble in water, and being able to be extracted from *S. cepivorum* by precipitation in an HCl solution [49,50]. The sclerotia and purified pigment were analyzed and, when comparing the spectrum data, we confirmed that the pigment covering the sclerotia and the purified pigment were the same (Figure 1).

The samples were analyzed at a resolution of  $4\text{ cm}^{-1}$  ( $4000\text{--}650\text{ cm}^{-1}$ ), obtaining the signals of the functional groups present in the extracted melanin (Table 1). Similar data were reported for *Phyllosticta capitalensis*, an endophytic fungus [51]. The signals between  $3300\text{--}3000\text{ cm}^{-1}$  helped to provide initial data about the type of melanin; if the DOPA-melanin route was carried out by *S. cepivorum*, we would have expected a sharp peak of medium intensity instead of the wide and high-intensity obtained peak (Figure 1C). Furthermore, in the DOPA-melanin route, nitrogen-linked carbon elongation strong intensity signals would have been expected for aromatic amine between  $1340\text{--}1260\text{ cm}^{-1}$ ; these were not observed. The signals presented between  $1410\text{--}1310\text{ cm}^{-1}$  and  $1260\text{--}1180\text{ cm}^{-1}$  were characteristic for phenol derivatives and referred to C-O stretching and H in plane deformations [28], giving a proposal of the DHN-melanin pathway. The DHN-melanin extracted from *Aspergillus fumigatus* [29] was analyzed by IR and compared with synthetic melanin. The same characteristic signals were reported for both samples; signals that were observed in our FTIR spectra. Regarding the possibility that it may have been pyomelanin, another substitution pattern would have been observed in the deformation signals in the in plane and outside this for the aromatic nucleus different from the 1:2:3 substitution. The characteristic signals of phenols and their derivatives also would not appear; therefore, the pyomelanin pathway was doubtful as the pyomelanin pathway is reported only in a few mushrooms and basidiomycetes [52]. Here, we were capable of assigning a molecular and bound functional group description to each peak (Table 1) and when comparing our data with the signals reported for *A. fumigatus* [29], we found similar peaks describing DHN-melanin. Furthermore, our IR melanin spectra differed from the eumelanin-reported spectra, specifically for the sharp shape in the  $3200\text{--}3000\text{ cm}^{-1}$  region [53]. At this point, the FTIR only partially suggested a tendency of DHN-melanin.  $^{13}\text{C}$  RMN was performed to support the FTIR data and the proposed DHN-melanin pathway.  $^{13}\text{C}$  RMN showed a chemical shift at 160.19 ppm and 135.77–111.32 ppm (Figure 2 and Table 2) as was reported by Raman and Ramasamy [29] for an *Aspergillus fumigates* DHN-extracted melanin. Table 2 also describes the chemical shifts corresponding with the chemical groups with nitrogen that are associated with chitin and related glucans but not with DOPA-melanin; therefore, an inhibition test was performed to support the data.

We performed the melanin inhibition test by using tricyclazole, a known inhibitor of the enzymatic reduction of trihydroxynaphthalene to vermeline, which are DHN-melanin pathway intermediates [50,54]. The inhibition assays showed that tricyclazole disturbed the normal development of the sclerotia, retarding the pigmentation process (Figure 3) and suggesting that tricyclazole affected the *S. cepivorum* melanogenic pathway, as reported in *Verticillium dahlia* with the same antifungal drug [54]. The observed delayed pigmentation was comprehensible because tricyclazole is a competitive inhibitor [55] and the fungus will produce the enzyme until the complete maturation of the sclerotia. Furthermore, the ANOVA analysis (Figure 4) indicated a significant difference between the treatments compared with the controls; therefore, a notorious effect existed on the development and melanization of *S. cepivorum* because of the tricyclazole. Additionally, we did not find in the genome of our *S. cepivorum* UGTO-Sc1 strain any genes related to the DOPA-melanin pathway such as tyrosinase (TYR), tyrosinase-related protein (TRP1), or dopachrome tautomerase (TRP2). At this point, we discarded the DOPA-melanin pathway and suggested that *S. cepivorum* used the DHN-melanin pathway for sclerotia melanization. Although tricyclazole has been used to control *M. grisea*, the side effects that it produces on the host such as accumulating on the plant leaves [56] makes the need to search for new strategies for the control of the disease urgent. The SDH enzyme represents a target for the development of new antifungal drugs.

The central role played by the genes that take part in the DHN melanogenic pathway of fungi makes them attractive candidates to study for the development of strategies that allow the control of phytopathogenic fungi. We identified the *sdh* gene from *S. cepivorum* in a typical biosynthetic gene cluster [57,58] and the arrangement of the genes was like that found in *S. sclerotiorum* (Ortega-Cuevas, [59]). The ORF *sdh* gene bioinformatic analysis indicated that the SDH was a protein of 167 aa with a molecular weight of 22.61 kDa (Figure 5). The *sdh* amino acid sequence was very similar between *S. cepivorum* and *S. sclerotiorum* (Supplementary Figure S4). Modeling on the platform swissmodel.expasy.org (data not shown) presented a similar structure to other reported fungi scytalone dehydratases [58]. The *S. cepivorum* *sdh* gene was analyzed and compared with the *sdh* gene of *S. sclerotiorum*, showing the differences between them such as the number and size of the introns of each gene as well as the size of the exons that comprise them (GenBank: SS1G\_13314 and MK965546.1).

In the absence of effective methods to transform *S. cepivorum*, we carried out the experiments with a recombinant enzyme as previously reported for *P. oryzae* [60]. Interestingly, the recombinant enzyme, expressed in *P. pastoris* X-33, showed activity against a fluorinated coumarin substrate (Figure 6). In addition, the recombinant protein had in its sequence the amino acid valine 75, which is responsible for the enzymatic activities of converting scytalone to 1,3,8-trihydroxynaphthalene, as reported in *M. oryzae* [50].

Here, the gene identification, expression, and activity of the SDH added relevant information for the melanin synthesis pathway of *S. cepivorum* and the members of this family of phytopathogens fungi. Finally, our data suggested that the *S. cepivorum* SDH took part in the melanization pathway. Knowledge of the enzymes involved in melanin biogenesis could be used to select an appropriate target for developing strategies against white rot plant disease.

## 5. Conclusions

The <sup>13</sup>C NMR and IR results, the bioinformatic results obtained, the determination of the presence of cDNA in the extracted RNA, and the expression of the enzymatic activity together with the results of the retardation of melanization by tricyclazole strongly suggested that the melanogenic route involved in *S. cepivorum* was the DHN pathway.

**Supplementary Materials:** The following are available online at <https://www.mdpi.com/article/10.3390/microbiolres13020013/s1>. File S1. Obtaining the Ethyl 2-hydroxy-2-(trifluoromethyl)-2H-chromene-3-carboxylate [61,62]. Supplementary Figure S1. Ethyl 2-hydroxy-2-(trifluoromethyl)-2H-chromene-3-carboxylate 1H NMR spectrum (500 MHz, CDCl<sub>3</sub>) δ: 1.42 (t, J = 7.2 Hz, 3H, CH<sub>3</sub>), 4.39

(q, J = 7.2 Hz, 2H, CH<sub>2</sub>), 7.02–7.06 (m, 2H), 7.26 (dd, J = 7.9, 1.7 Hz, 1H), 7.39 (m, 1H), 7.45 (s, 1H, OH), 7.79 (s, 1H). Supplementary Figure S2. Ethyl 2-hydroxy-2-(trifluoromethyl)-2H-chromene-3-carboxylate <sup>13</sup>C-NMR spectrum (CDCl<sub>3</sub>, 125 MHz) δ: 14.1 (CH<sub>3</sub>), 62.4 (CH<sub>2</sub>), 95.3 (q, J<sub>C,F</sub> = 34.8 Hz, CCF<sub>3</sub>), 114.8, 116.0, 117.6, 121.5 (q, J<sub>C,F</sub> = 290 Hz, CF<sub>3</sub>), 122.7, 129.5, 133.9, 139.3, 152.7, 166.8 (C=O). Supplementary Figure S3. Ethyl 2-hydroxy-2-(trifluoromethyl)-2H-chromene-3-carboxylate HMQS spectrum of 2D-NMR (CDCl<sub>3</sub>). Supplementary Figure S4. *Sclerotinia sclerotiorum* alignment. Comparison between SDH of *Sclerotinia sclerotiorum* (Sequence ID: EDN98455.1) and another SDH of different size. NCBI alignment. Supplementary Figure S5. Multiple alignment of the Scytalone dehydratase gene from *Sclerotium cepivorum* in Gene Bank; NGKD01000004.1 genome sequenced by Kohn., RCTD01000004.1 genome sequenced by Valero-Jimenez et al. [63] and MK965546.1 complete SDH cds. Supplementary Figure S6. Distance tree SDH of *S. cepivorum* UGTO-Sc1 (GenBank: MK965546.1) [64]. Supplementary Figure S7. Phylogenetic tree of *S. cepivorum* UGTO-Sc1 SDH [65–71]. Supplementary Figure S8. *Sclerotinia sclerotiorum* alignment. Comparison between SDH of *Sclerotinia sclerotiorum* (Sequence ID: EDN98455.1) and another SDH of different size. NCBI alignment. Supplementary Table S1. Primers used for the expression of the SDH heterologous protein. Expression performed in *Pichia pastoris* by using a pPICZα plasmid (Invitrogen™).

**Author Contributions:** Conceptualization, L.M.S.-G. and P.P.-N.; methodology, L.M.S.-G., R.I.O.-C., R.A.M.-Á., J.A.M.-Á. and S.E.G.-H.; analytical experiments, L.M.S.-G., D.M.-O. and M.Á.V.; formal analysis, A.F.-M., L.M.S.-G., D.M.-O., M.Á.V. and P.P.-N.; investigation, A.F.-M., L.M.S.-G. and P.P.-N.; resources, A.F.-M. and P.P.-N.; data curation, L.M.S.-G., R.I.O.-C., A.F.-M. and P.P.-N.; writing-original draft preparation, L.M.S.-G.; writing-review and editing, L.M.S.-G., A.F.-M., M.Á.V. and P.P.-N.; supervision, S.E.G.-H., J.A.M.-Á., P.P.-N. and A.F.-M.; project administration, S.E.G.-H. and P.P.-N.; funding acquisition, A.F.-M. and P.P.-N. All authors contributed to the article and approved the submitted version. All authors have read and agreed to the published version of the manuscript.

**Funding:** This work was supported by funding from CONACYT-SAGARPA (2005-11919) and Dirección de Apoyo a la Investigación y al Posgrado (DAIP-UG: 2019,2020), Universidad de Guanajuato.

**Institutional Review Board Statement:** Not applicable.

**Informed Consent Statement:** Not applicable.

**Acknowledgments:** Luis M. Salazar-García (788756) and Rocío I. Ortega-Cuevas (520959) acknowledge support from CONACYT scholarships. We are grateful to Fernando Amézquita López and Laboratorio de Análisis Instrumental, DCNE, UGTO, for the analytical equipment time provided, and to Daniel Ruiz Plaza from Laboratorio Nacional de Caracterización de Propiedades Físicoquímicas y de Estructura Molecular (LACAPFEM) de la Universidad de Guanajuato as well as Sebastien Santini (CNRS/AMU IGS UMR7256) and the PACA Bioinfo platform (supported by IBISA) for the availability and management of the phylogeny.fr website used for the phylogenetic tree development.

**Conflicts of Interest:** The authors declare that the research was conducted in the absence of any commercial or financial relationships that could be construed as a potential conflict of interest.

## References

1. Coley-Smith, J.; King, J. The production by species of *Allium* of alkyl sulphides and their effect on germination of sclerotia of *Sclerotium cepivorum* Berk. *Ann. Appl. Biol.* **1969**, *64*, 289–301. [\[CrossRef\]](#)
2. Coley-Smith, J. White rot disease of *Allium*: Problems of soil-borne diseases in microcosm. *Plant Pathol.* **1990**, *39*, 214–222. [\[CrossRef\]](#)
3. Willetts, H.; Bullock, S. Developmental biology of sclerotia. *Mycol. Res.* **1992**, *96*, 801–816. [\[CrossRef\]](#)
4. Coley-Smith, J.R.; Parfitt, D. Some effects of diallyl bisulphide on sclerotia of *Sclerotium cepivorum*: Possible novel control method for white rot disease of onions. *Pestic. Sci.* **1986**, *17*, 587–594. [\[CrossRef\]](#)
5. Fullerton, R.; Stewart, A. Chemical control of onion white rot (*Sclerotium cepivorum* Berk.) in the Pukekohe district of New Zealand. *N. Z. J. Crop Hortic. Sci.* **1991**, *19*, 121–127. [\[CrossRef\]](#)
6. Entwistle, A. *Allium* white rot and its control. *Soil Use Manag.* **1990**, *6*, 201–208. [\[CrossRef\]](#)
7. Butler, M.J.; Gardiner, R.B.; Day, A.W. Melanin synthesis by *Sclerotinia sclerotiorum*. *Mycologia* **2009**, *101*, 296–304. [\[CrossRef\]](#)
8. Cordero, R.J.; Casadevall, A. Functions of fungal melanin beyond virulence. *Fungal Biol. Rev.* **2017**, *31*, 99–112. [\[CrossRef\]](#)
9. Arazoe, T.; Miyoshi, K.; Yamato, T.; Ogawa, T.; Ohsato, S.; Arie, T.; Kuwata, S. Tailor-made CRISPR/Cas system for highly efficient targeted gene replacement in the rice blast fungus. *Biotechnol. Bioeng.* **2015**, *112*, 2543–2549. [\[CrossRef\]](#)
10. Carbone, I.; Kohn, L.M. Ribosomal DNA sequence divergence within internal transcribed spacer 1 of the Sclerotiniaceae. *Mycologia* **1993**, *85*, 415–427. [\[CrossRef\]](#)

11. Xu, Z.; Harrington, T.C.; Gleason, M.L.; Batzer, J.C. Phylogenetic placement of plant pathogenic *Sclerotium* species among teleomorph genera. *Mycologia* **2010**, *102*, 337–346. [[CrossRef](#)] [[PubMed](#)]
12. Liang, Y.; Xiong, W.; Steinkellner, S.; Feng, J. Deficiency of the melanin biosynthesis genes SCD1 and THR1 affects sclerotial development and vegetative growth, but not pathogenicity, in *Sclerotinia sclerotiorum*. *Mol. Plant Pathol.* **2018**, *19*, 1444–1453. [[CrossRef](#)] [[PubMed](#)]
13. Eisenman, H.C.; Casadevall, A. Synthesis and assembly of fungal melanin. *Appl. Microbiol. Biotechnol.* **2012**, *93*, 931–940. [[CrossRef](#)] [[PubMed](#)]
14. Mattoon, E.R.; Cordero, R.J.; Casadevall, A. Fungal Melanins and Applications in Healthcare, Bioremediation and Industry. *J. Fungi* **2021**, *7*, 488. [[CrossRef](#)]
15. Langfelder, K.; Streibel, M.; Jahn, B.; Haase, G.; Brakhage, A.A. Biosynthesis of fungal melanins and their importance for human pathogenic fungi. *Fungal Genet. Biol.* **2003**, *38*, 143–158. [[CrossRef](#)]
16. Miñambres, G.G.; Conles, M.Y.; Lucini, E.I.; Verdenelli, R.A.; Meriles, J.M.; Zygadlo, J.A. Application of thymol and iprodione to control garlic white rot (*Sclerotium cepivorum*) and its effect on soil microbial communities. *World J. Microbiol. Biotechnol.* **2010**, *26*, 161. [[CrossRef](#)]
17. Wheeler, M.H.; Bell, A.A. Melanins and their importance in pathogenic fungi. In *Current Topics in Medical Mycology*; Springer: Berlin/Heidelberg, Germany, 1988; pp. 338–387.
18. Saitoh, Y.; Izumitsu, K.; Morita, A.; Tanaka, C.; Shimizu, K. Cloning of Sal1, a scytalone dehydratase gene involved in melanin biosynthesis in *Cochliobolus heterostrophus*. *Mycoscience* **2012**, *53*, 330–334. [[CrossRef](#)]
19. Sezonov, G.; Joseleau-Petit, D.; d’Ari, R. *Escherichia coli* physiology in Luria-Bertani broth. *J. Bacteriol.* **2007**, *189*, 8746–8749. [[CrossRef](#)]
20. Gadd, G. Effects of media composition and light on colony differentiation and melanin synthesis in *Microdochium bolleyi*. *Trans. Br. Mycol. Soc.* **1982**, *78*, 115–122. [[CrossRef](#)]
21. Froyd, J.; Paget, C.; Guse, L.; Dreikorn, B.; Pafford, J. Tricyclazole: A new systemic fungicide for control of *Pyricularia oryzae* on rice. *Phytopathology* **1976**, *66*, 1135–1139. [[CrossRef](#)]
22. Raeder, U.; Broda, P. Rapid preparation of DNA from filamentous fungi. *Lett. Appl. Microbiol.* **1985**, *1*, 17–20. [[CrossRef](#)]
23. Trujillo-Esquivel, E.; Franco, B.; Flores-Martínez, A.; Ponce-Noyola, P.; Mora-Montes, H.M. Purification of single-stranded cDNA based on RNA degradation treatment and adsorption chromatography. *Nucleosides Nucleotides Nucleic Acids* **2016**, *35*, 404–409. [[CrossRef](#)] [[PubMed](#)]
24. Laemmli, U.K. Cleavage of structural proteins during the assembly of the head of bacteriophage T4. *Nature* **1970**, *227*, 680–685. [[CrossRef](#)] [[PubMed](#)]
25. Wheeler, M.H. Comparisons of fungal melanin biosynthesis in ascomycetous, imperfect and basidiomycetous fungi. *Trans. Br. Mycol. Soc.* **1983**, *81*, 29–36. [[CrossRef](#)]
26. Simon, W.; Clerc, T. *Elucidación Estructural de Compuestos Orgánicos por Métodos Espectroscópicos*; Alhambra: Madrid, Spain, 1970.
27. Rajagopal, K.; Kathiravan, G.; Karthikeyan, S. Extraction and characterization of melanin from *Phomopsis*: A phelloglyphic fungi isolated from *Azadirachta indica* A. Juss. *Afr. J. Microbiol. Res.* **2011**, *5*, 762–766.
28. Pretsch, E.; Clerc, T.; Seibl, J.; Simon, W. *Tables of Spectral Data for Structure Determination of Organic Compounds*; Springer Science & Business Media: Berlin/Heidelberg, Germany, 2013.
29. Raman, N.M.; Ramasamy, S. Genetic validation and spectroscopic detailing of DHN-melanin extracted from an environmental fungus. *Biochem. Biophys. Rep.* **2017**, *12*, 98–107. [[CrossRef](#)]
30. Manini, P.; Lino, V.; D’Errico, G.; Reale, S.; Napolitano, A.; De Angelis, F.; d’Ischia, M. “Blackness” is an index of redox complexity in melanin polymers. *Polym. Chem.* **2020**, *11*, 5005–5010. [[CrossRef](#)]
31. Chatterjee, S.; Prados-Rosales, R.; Itin, B.; Casadevall, A.; Stark, R.E. Solid-state NMR reveals the carbon-based molecular architecture of *Cryptococcus neoformans* fungal eumelanins in the cell wall. *J. Biol. Chem.* **2015**, *290*, 13779–13790. [[CrossRef](#)]
32. Kang, X.; Kirui, A.; Muszyński, A.; Widanage, M.C.D.; Chen, A.; Azadi, P.; Wang, P.; Mentink-Vigier, F.; Wang, T. Molecular architecture of fungal cell walls revealed by solid-state NMR. *Nat. Commun.* **2018**, *9*, 1–12. [[CrossRef](#)]
33. Di Pietro, M.E.; Mannu, A.; Mele, A. NMR determination of free fatty acids in vegetable oils. *Processes* **2020**, *8*, 410. [[CrossRef](#)]
34. Zhang, C.-Q.; Huang, X.; Wang, J.-X.; Zhou, M.-G. Resistance development in rice blast disease caused by *Magnaporthe grisea* to tricyclazole. *Pestic. Biochem. Physiol.* **2009**, *94*, 43–47. [[CrossRef](#)]
35. Butler, M.; Day, A. Fungal melanins: A review. *Can. J. Microbiol.* **1998**, *44*, 1115–1136. [[CrossRef](#)]
36. Amselem, J.; Cuomo, C.A.; van Kan, J.A.; Viaud, M.; Benito, E.P.; Couloux, A.; Coutinho, P.M.; de Vries, R.P.; Dyer, P.S.; Fillinger, S. Genomic analysis of the necrotrophic fungal pathogens *Sclerotinia sclerotiorum* and *Botrytis cinerea*. *PLoS Genet.* **2011**, *7*, e1002230. [[CrossRef](#)]
37. Jordan, D.B.; Basarab, G.S.; Steffens, J.J.; Lundqvist, T.; Pfrogner, B.R.; Schwartz, R.S.; Wawrzak, Z. Catalytic mechanism of scytalone dehydratase from *Magnaporthe grisea*. *Pestic. Sci.* **1999**, *55*, 277–280. [[CrossRef](#)]
38. Tsuji, G.; Takeda, T.; Furusawa, I.; Horino, O.; Kubo, Y. Carpropamid, an Anti-Rice Blast Fungicide, Inhibits Scytalone Dehydratase Activity and Appressorial Penetration in *Colletotrichum lagenarium*. *Pestic. Biochem. Physiol.* **1997**, *57*, 211–219. [[CrossRef](#)]
39. Liachko, I.; Youngblood, R.A.; Tsui, K.; Bubbs, K.L.; Queitsch, C.; Raghuraman, M.; Nislow, C.; Brewer, B.J.; Dunham, M.J. GC-rich DNA elements enable replication origin activity in the methylotrophic yeast *Pichia pastoris*. *PLoS Genet.* **2014**, *10*, e1004169. [[CrossRef](#)] [[PubMed](#)]

40. Lundqvist, T.; Rice, J.; Hodge, C.N.; Basarab, G.S.; Pierce, J.; Lindqvist, Y. Crystal structure of scytalone dehydratase—A disease determinant of the rice pathogen, *Magnaporthe grisea*. *Structure* **1994**, *2*, 937–944. [[CrossRef](#)]
41. Allam, N.G.; El-Zaher, E.A. Protective role of *Aspergillus fumigatus* melanin against ultraviolet (UV) irradiation and Bjerkandera adusta melanin as a candidate vaccine against systemic candidiasis. *Afr. J. Biotechnol.* **2012**, *11*, 6566–6577.
42. Potgieter, H.; Alexander, M. Susceptibility and resistance of several fungi to microbial lysis. *J. Bacteriol.* **1966**, *91*, 1526–1532. [[CrossRef](#)]
43. Chumley, F.G.; Valent, B. Genetic analysis of melanin-deficient, nonpathogenic mutants of *Magnaporthe grisea*. *Mol. Plant-Microbe Interact* **1990**, *3*, 135–143. [[CrossRef](#)]
44. Mahmoud, Y.A.; Sammour, R.H.; Mustafa, A.-Z.M.; Alhozeim, R.A. Role of sclerotia in the aggressiveness and pathogenicity of *Sclerotium cepivorum*. *Asian J. Microbiol. Biotechnol. Environ. Sci.* **2021**, *23*, 16–23.
45. Moriwaki, A.; Kihara, J.; Kobayashi, T.; Tokunaga, T.; Arase, S.; Honda, Y. Insertional mutagenesis and characterization of a polyketide synthase gene (PKS1) required for melanin biosynthesis in *Bipolaris oryzae*. *FEMS Microbiol. Lett.* **2004**, *238*, 1–8. [[PubMed](#)]
46. Rehnstrom, A.; Free, S. The isolation and characterization of melanin-deficient mutants of *Monilinia fructicola*. *Physiol. Mol. Plant Pathol.* **1996**, *49*, 321–330. [[CrossRef](#)]
47. Thines, E.; Heidrun, A.; Weber, R.W. Fungal secondary metabolites as inhibitors of infection-related morphogenesis in phytopathogenic fungi. *Mycol. Res.* **2004**, *108*, 14–25. [[CrossRef](#)]
48. Bell, A.A.; Wheeler, M.H. Biosynthesis and functions of fungal melanins. *Annu. Rev. Phytopathol.* **1986**, *24*, 411–451. [[CrossRef](#)]
49. De la Rosa, J.M.; Martin-Sanchez, P.M.; Sanchez-Cortes, S.; Hermosin, B.; Knicker, H.; Saiz-Jimenez, C. Structure of melanins from the fungi *Ochroconis lascauxensis* and *Ochroconis anomala* contaminating rock art in the Lascaux Cave. *Sci. Rep.* **2017**, *7*, 13441. [[CrossRef](#)]
50. Pal, A.K.; Gajjar, D.U.; Vasavada, A.R. DOPA and DHN pathway orchestrate melanin synthesis in *Aspergillus* species. *Med. Mycol.* **2014**, *52*, 10–18.
51. Suryanarayanan, T.S.; Ravishankar, J.P.; Venkatesan, G.; Murali, T.S. Characterization of the melanin pigment of a cosmopolitan fungal endophyte. *Mycol. Res.* **2004**, *108*, 974–978. [[CrossRef](#)]
52. Solano, F. Melanins: Skin pigments and much more—Types, structural models, biological functions, and formation routes. *New J. Sci.* **2014**, *2014*, 498276. [[CrossRef](#)]
53. Correa, N.; Covarrubias, C.; Rodas, P.I.; Hermosilla, G.; Olate, V.R.; Valdés, C.; Meyer, W.; Magne, F.; Tapia, C.V. Differential antifungal activity of human and cryptococcal melanins with structural discrepancies. *Front. Microbiol.* **2017**, *8*, 1292. [[CrossRef](#)]
54. Tokousbalides, M.C.; Sisler, H. Site of inhibition by tricyclazole in the melanin biosynthetic pathway of *Verticillium dahliae*. *Pestic. Biochem. Physiol.* **1979**, *11*, 64–73. [[CrossRef](#)]
55. Andersson, A.; Jordan, D.; Schneider, G.; Lindqvist, Y. Crystal structure of the ternary complex of 1, 3, 8-trihydroxynaphthalene reductase from *Magnaporthe grisea* with NADPH and an active-site inhibitor. *Structure* **1996**, *4*, 1161–1170. [[CrossRef](#)]
56. Liu, J.; Min, H.; Ye, L. The negative interaction between the degradation of phenanthrene and tricyclazole in medium, soil and soil/compost mixture. *Biodegradation* **2008**, *19*, 695–703. [[CrossRef](#)]
57. Keller, N.P. Fungal secondary metabolism: Regulation, function and drug discovery. *Nat. Rev. Microbiol.* **2019**, *17*, 167–180. [[CrossRef](#)] [[PubMed](#)]
58. Jia, S.-L.; Chi, Z.; Chen, L.; Liu, G.-L.; Hu, Z.; Chi, Z.-M. Molecular evolution and regulation of DHN melanin-related gene clusters are closely related to adaptation of different melanin-producing fungi. *Genomics* **2021**, *113*, 1962–1975. [[CrossRef](#)] [[PubMed](#)]
59. Ortega-Cuevas, R.I. Clonación y Expresión Heteróloga de la Scitalona Deshidratasa de *Sclerotium Cepivorum Berk*. Master's Thesis, Department of Biology, University of Guanajuato, Guanajuato, Mexico, 2015.
60. Yamada, N.; Motoyama, T.; Nakasako, M.; Kagabu, S.; Kudo, T.; Yamaguchi, I. Enzymatic characterization of scytalone dehydratase Val75Met variant found in melanin biosynthesis dehydratase inhibitor (MBI-D) resistant strains of the rice blast fungus. *Biosci. Biotechnol. Biochem.* **2004**, *68*, 615–621. [[CrossRef](#)] [[PubMed](#)]
61. Chizhov, D.L.; Sosnovskikh, V.Y.; Pryadeina, M.V.; Burgart, Y.V.; Saloutin, V.I.; Charushin, V.N. The first synthesis of 4-unsubstituted 3-(trifluoroacetyl) coumarins by the Knoevenagel condensation of salicylaldehydes with ethyl trifluoroacetate followed by chromene-coumarin recyclization. *Synlett* **2008**, *19*, 281–285. [[CrossRef](#)]
62. Xu, C.; Yang, G.; Wang, C.; Fan, S.; Xie, L.; Gao, Y. An efficient solvent-free synthesis of 2-hydroxy-2-(trifluoromethyl)-2H-chromenes using silica-immobilized L-proline. *Molecules* **2013**, *18*, 11964–11977. [[CrossRef](#)]
63. Valero-Jiménez, C.A.; Steentjes, M.B.; Slot, J.C.; Shi-Kunne, X.; Scholten, O.E.; van Kan, J.A. Dynamics in Secondary Metabolite Gene Clusters in Otherwise Highly Syntenic and Stable Genomes in the Fungal Genus. *Genome Biol. Evol.* **2020**, *12*, 2491–2507.
64. Zhang, Z.; Schwartz, S.; Wagner, L.; Miller, W. A greedy algorithm for aligning DNA sequences. *J. Comput. Biol.* **2000**, *7*, 203–214. [[CrossRef](#)]
65. Dereeper, A.; Audic, S.; Claverie, J.M.; Blanc, G. BLAST-EXPLORER helps you building datasets for phylogenetic analysis. *BMC Evol. Biol.* **2010**, *10*, 8. [[CrossRef](#)]
66. Dereeper, A.; Guignon, V.; Blanc, G.; Audic, S.; Buffet, S.; Chevenet, F.; Dufayard, J.F.; Guindon, S.; Lefort, V.; Lescot, M.; et al. Phylogeny.fr: Robust phylogenetic analysis for the non-specialist. *Nucleic Acids Res.* **2008**, *36*, W465–W469. [[CrossRef](#)] [[PubMed](#)]
67. Edgar, R.C. MUSCLE: Multiple sequence alignment with high accuracy and high throughput. *Nucleic Acids Res.* **2004**, *32*, 1792–1797. [[CrossRef](#)] [[PubMed](#)]

68. Castresana, J. Selection of conserved blocks from multiple alignments for their use in phylogenetic analysis. *Mol. Biol. Evol.* **2000**, *17*, 540–552. [[CrossRef](#)] [[PubMed](#)]
69. Guindon, S.; Gascuel, O. A simple, fast, and accurate algorithm to estimate large phylogenies by maximum likelihood. *Syst. Biol.* **2003**, *52*, 696–704. [[CrossRef](#)] [[PubMed](#)]
70. Anisimova, M.; Gascuel, O. Approximate likelihood ratio test for branches: A fast, accurate and powerful alternative. *Syst. Biol.* **2006**, *55*, 539–552. [[CrossRef](#)]
71. Chevenet, F.; Brun, C.; Banuls, A.L.; Jacq, B.; Chisten, R. TreeDyn: Towards dynamic graphics and annotations for analyses of trees. *BMC Bioinform.* **2006**, *7*, 439. [[CrossRef](#)]